

## Reciprocating pipe flows as a model of high-frequency ventilation

J. S. Leontini<sup>1</sup>, M. K. Hasan<sup>1</sup>, M. D. Griffith<sup>1</sup>, R. Swain<sup>1</sup> and R. Manasseh<sup>1</sup>

<sup>1</sup>Faculty of Science, Engineering and Technology  
Swinburne University of Technology, Victoria 3122, Australia

### Abstract

High-frequency ventilation is a strategy primarily used to provide oxygen to neonatal patients in intensive care. Here, a simple model of the reciprocating flow in a straight pipe with a free end exiting into a large reservoir is examined to investigate some of the fluid mechanics present during high-frequency ventilation. The resulting recirculating mean flow is quantified in terms of the amount of mean recirculating flux and the distance from the free end to which this recirculation penetrates.

### Introduction

High-frequency ventilation (HFV) is a method of providing oxygen to patients in intensive care. In particular, it is used in neonatal intensive care units (NICU) for critically ill babies. During HFV, the patient is completely sedated and intubated, with gases supplied and removed via an endotracheal tube (a tube inserted via the throat into the trachea). A purported advantage of HFV over traditional ventilation is its protection of damaged or otherwise-delicate lungs and airways. This protective capacity comes from the fact that HFV uses fast, small inflations - usual values are frequencies around 10Hz and volumes per inflation from 1ml to 10ml [3, 2]. These small volumes of inflation mean that peak pressures in the airway and lungs are minimized, hence reducing the risk of lung damage via over-distension.

However, these small volumes of inhalation - which at their greatest are  $< 10\%$  of the “dead space” volume of the airway - raise interesting questions from a fluid mechanics perspective. Gas transport (oxygen down, carbon dioxide up) is not achieved by bulk advection, or emptying and filling the lungs, but by other more subtle mechanisms. Some of these potential mechanisms, as outlined by Slutsky & Brown [7] and Standiford [8] include turbulent convection in the upper airway, Taylor dispersion [9, 1], and nonlinear streaming.

Further fundamental understanding of these mechanisms can help address outstanding clinical problems such as

- finding optimal settings for a specific patient
- extending the success of HFV and its lung protective capacity to adults [6].

Nonlinear mean streaming (the focus of this paper) occurs in reciprocating flow such as those in the airway due to presence of spatial gradients in the flow. These spatial gradients mean that even though the flow in the airway has a zero net mass flux (the same amount of flow goes in and out over one inflation cycle) the mean flow at a particular location is non-zero. For both of these facts to be true, a mean recirculating flow needs to occur, and it is this mean recirculation that can transport gases up and down the airway.

The human airway is essentially a set of connected bifurcating pipes. Here, a very simple model flow is examined, the reciprocating flow in a straight pipe with a free end exiting into a

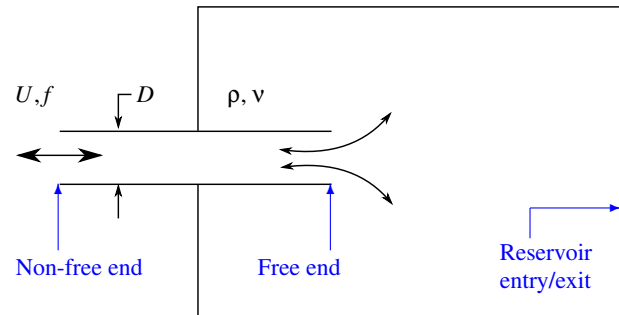


Figure 1: A schematic of the basic problem setup investigated. A time-dependent boundary condition is applied at the non-free end, and the free end acts as an exit/entry to/from a large reservoir.

large reservoir. Flow separation and subsequent vortex production lead to large local gradients and therefore mean streaming. The recirculating flux, and the distance from the free end down the pipe which this recirculating flow extends is quantified, to investigate if optimum quantities can be found and related to the underlying flow features.

### Methodology

Axisymmetric simulations of the sinusoidally reciprocating flow in a horizontal straight pipe with a free end exiting into a reservoir were conducted using a highly-validated spectral-element code [10, 5] solving the incompressible Navier–Stokes equations. A schematic of the basic problem setup is shown in figure 1. At the non-free end, an oscillatory boundary condition of a set frequency  $f$  and peak cross-sectional-mean velocity  $U$  was imposed such that the flow matched the analytic solution for the reciprocating flow in an infinitely long pipe [11]. At the pipe walls and lateral reservoir boundaries, a no-slip condition was applied. At the exit/entry to the reservoir, a time-dependent Poiseuille profile was imposed, the instantaneous amplitude of which was set so that the flow rate in/out of the reservoir matched the flow rate out/in of the non-free end. At all boundaries, the normal pressure gradient was set to zero.

Ignoring the length of the pipe (assuming it is long enough that flow returns to the fully-developed solution at some distance from the free end) the flow is a function of two dimensionless parameters, here defined as the maximum Reynolds number  $Re_{\max} = UD/\nu$  (essentially a dimensionless amplitude), and the oscillatory Reynolds number  $\alpha' = 2\pi f D^2/\nu$  (essentially a dimensionless frequency), where  $U$  is the amplitude of the cross-sectional-mean velocity in the pipe,  $D$  is the pipe diameter,  $\nu$  is the fluid kinematic viscosity, and  $f$  is the imposed frequency.

Note the oscillatory Reynolds number can be interpreted as a ratio of lengths. The Stokes layer thickness  $\delta = \sqrt{2\nu/(2\pi f)}$  is the thickness of the oscillatory boundary layer in the pipe, and so  $\alpha'$  can be defined as  $\alpha' = 8(\Lambda)^2$ , where  $\Lambda = D/(2\delta)$  is the traditional Stokes parameter, or the ratio of the pipe radius to the Stokes layer thickness. Similarly, if  $\delta$  is taken as the

length scale, an alternative Reynolds number  $Re_\delta = U\delta/\nu$  can be defined. Both of these alternative parameters are used to analyze results in the following sections.

## Results

Of primary interest is the amount of flow that is recirculated, and how far down the pipe this recirculation penetrates. The amount of flow recirculated is quantified by integrating the mean velocity field over the portion of the plane covering the end of the pipe through which the flux is positive,

$$q = \int \bar{\mathbf{u}} \cdot \hat{\mathbf{n}} H(\bar{\mathbf{u}} \cdot \hat{\mathbf{n}}) dA \quad (1)$$

where  $H$  is the Heaviside function. This mean flow rate is then normalized as  $Q^* = 4q/(\pi UD^2)$  (divided by the maximum flowrate).

The length of this recirculating flow is quantified by the recirculation length  $L$ , defined here as the distance from the free end of the pipe at which the mean axial velocity on the pipe centreline does not vary with further increases in distance. In practice, this is taken as the point at which the absolute value of  $\partial \bar{u}_{r0}/\partial x$  falls below some small threshold, here taken as 0.0005.

Figure 2(a) shows the normalised recirculation length  $L/D$  as a function of  $Re_{\max}$ , where  $D$  has been taken as the relevant length scale. Results are shown for nine values of  $\Lambda$ . The figure shows that while  $\Lambda < 2.5$ , the normalized length  $L/D$  is essentially independent of  $\Lambda$  and increases linearly with  $Re_{\max}$ . Figure 2(b) shows the same data, but here  $\delta$  has been taken as the relevant length scale, plotting the normalised recirculation length  $L/\delta$  as a function of  $Re_\delta$ . Here it is clear that for  $\Lambda \geq 2.5$ , the normalized length  $L/\delta$  is independent of  $\Lambda$  and increases linearly with  $Re_\delta$ . These results suggest two primary flow regimes as a function of the Stokes parameter  $\Lambda$ : a low  $\Lambda$  regime, where the relevant length scale is the pipe diameter  $D$ ; and a high  $\Lambda$  regime, where the relevant length scale is the Stokes layer thickness  $\delta$ .

This hypothesis is further refined by plotting the normalized flow rate  $Q^*$  as a function of  $Re_{\max}$ , as presented in figure 2(c). It is shown that  $Q^*$  is almost independent of  $\Lambda$  for  $\Lambda < 2.5$ , with the results for all the amplitudes tested collapsing to a single curve with a local maxima of  $Q^* \simeq 0.06$  occurring at  $Re_{\max} \simeq 300$ . For higher values of  $\Lambda > 6$ ,  $Q^*$  appears to collapse to a single weak linear function of  $Re_{\max}$ . However, there is also an intermediate  $\Lambda$  regime between these two extremes, where  $Q^*$  is clearly a function of both  $\Lambda$  and  $Re_{\max}$ . In this intermediate regime, the maximum flow rate decreases with increasing  $\Lambda$ .

Figure 3 shows an example of the mean flow generated, here for  $Re_{\max} = 800$ ,  $\Lambda = 2.24$ . The mean vorticity in one half plane inside the pipe is shown, clearly illustrating the recirculating nature of the flow by the change in sign of vorticity as the pipe is traversed in the radial direction. The mean axial velocity on the pipe centreline is shown, showing that at a certain distance from the free end the mean flow returns to zero (at a distance  $x \simeq 10$  in the figure). Also shown is the mean axial velocity profile across the very end of the pipe. The regions used to calculate the mean recirculating flux are shaded.

The idea that the collapse of the data in the low and high  $\Lambda$  regime is related to a change in the dominant length scale is further investigated in figure 4. Here, instantaneous snapshots of the axial velocity profile across the end of the pipe are plotted at 8 phases throughout the oscillation cycle, from a high  $\Lambda$  example ( $Re_{\max} = 2400$ ,  $\Lambda = 7.07$ ), and a low  $\Lambda$  example close to the optimum for flow rate ( $Re_{\max} = 240$ ,  $\Lambda = 2.24$ ).

The plots show the change in relevant length scale. In the high

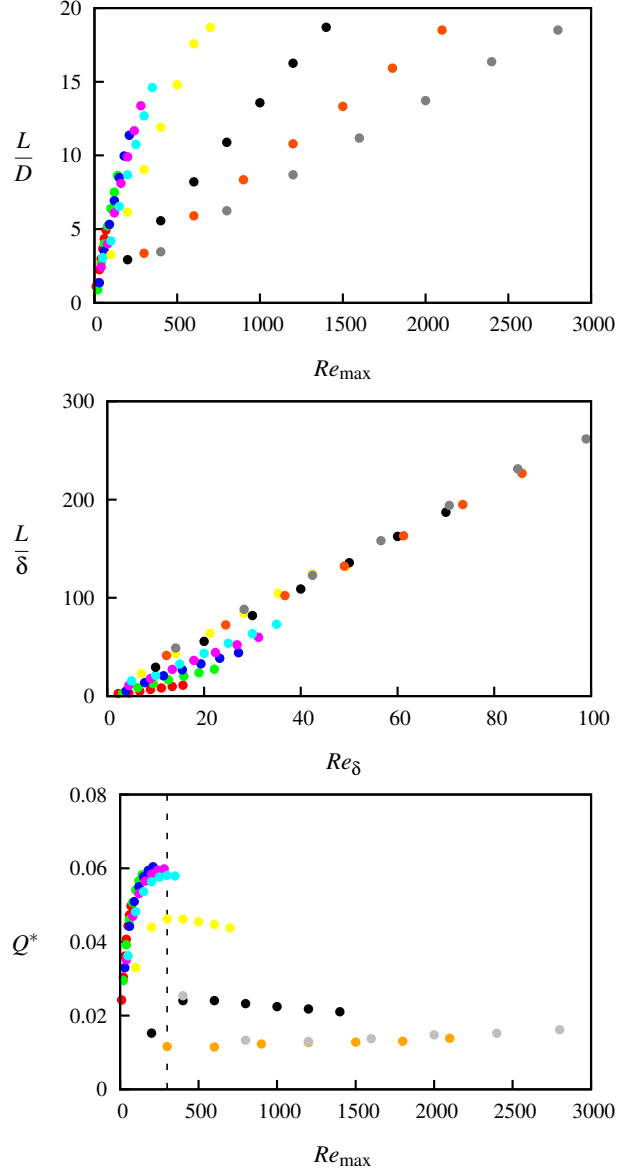


Figure 2: (a) Recirculation length  $L$  normalized by pipe diameter  $D$  as a function of  $Re_{\max}$ . (b) The same data as (a), but  $L$  is normalized by the Stokes layer thickness  $\delta$ . (c) Normalized flow rate as a function of  $Re_{\max}$ . The dashed line marks the value of  $Re_{\max}$  of the apparent optimum for flow rate. Colours of points represent values of  $\Lambda$ :  $\bullet$ ,  $\Lambda = 1.12$ ;  $\bullet$ ,  $\Lambda = 1.58$ ;  $\bullet$ ,  $\Lambda = 1.94$ ;  $\bullet$ ,  $\Lambda = 2.24$ ;  $\bullet$ ,  $\Lambda = 2.50$ ;  $\bullet$ ,  $\Lambda = 3.54$ ;  $\bullet$ ,  $\Lambda = 5.00$ ;  $\bullet$ ,  $\Lambda = 6.12$ ;  $\bullet$ ,  $\Lambda = 7.07$

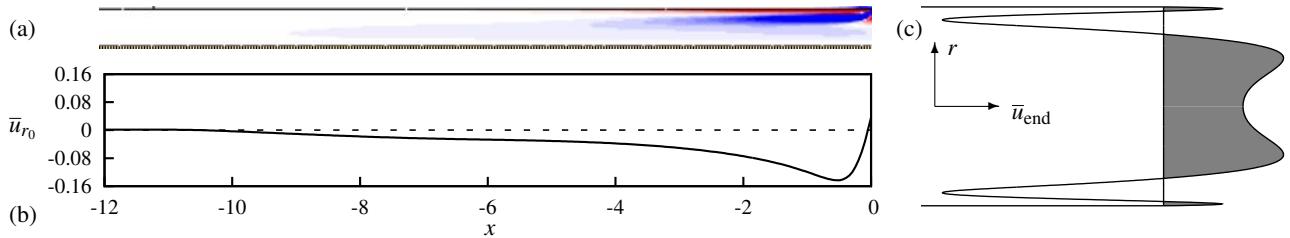


Figure 3: Example measurements of the mean flow for  $Re_{\max} = 800$ ,  $\Lambda = 2.24$ . (a) Contours of mean normalised vorticity  $\Omega = \omega D / U$  (where  $\omega$  is the vorticity with vector out of the plane of the page) in the upper half of the centre plane. Blue/red contours represent positive/negative vorticity. Contour levels are between  $\Omega = \pm 1$ . (b) Mean axial velocity on the centre line of the pipe, near the free end. Note that for the length scale  $x = 0$  is at the free end of the pipe, and  $x$  is made non-dimensional with  $D$ . (c) The mean velocity profile across the end of the pipe, with the shaded region showing the portions used to find the mean recirculating flux.

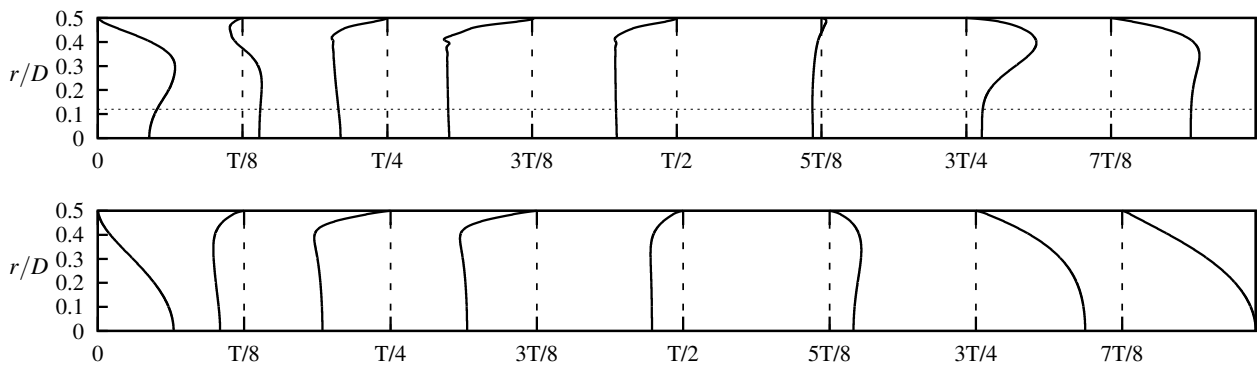


Figure 4: Snapshots of axial velocity profiles, taken at the free end of the pipe, at different phases of oscillation over one period  $T$  for (a)  $Re_{\max} = 2400$ ,  $\Lambda = 7.07$  as an example of the high  $\Lambda$  regime and (b)  $Re_{\max} = 240$ ,  $\Lambda = 2.24$  as an example of the low  $\Lambda$  regime. In the high  $\Lambda$  regime, all the profiles are essentially flat for  $r/D < 0.12$  (marked with the fine dashed line) indicating little interaction between the Stokes layers on each side. In the low  $\Lambda$  regime, some profiles are essentially parabolic indicating each side is interacting.

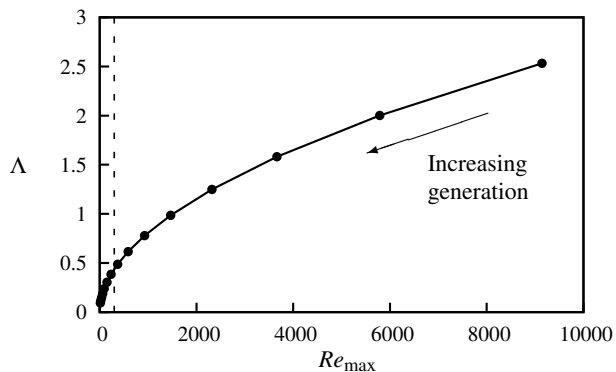


Figure 5: Values of  $Re_{max}$  and  $\Lambda$  for each generation from 1 to 15 of an example infant airway, using the scaling of Grotberg [2]. Each point represents an airway generation. Practically all generations are approaching the low  $\Lambda$  regime, and generations 8 and 9 are close to the optimum value of  $Re_{max}$  for maximizing flux (marked with the dashed line) according to the data plotted in figure 2(c).

$\Lambda$  example, the profiles exiting and entering the pipe are flat through the entire period in the middle of the pipe, for a radius  $r < 0.12$ . However, in the low  $\Lambda$  regime, this flat section is not observed, highlighting the interaction of the Stokes layers, and vortex structures that form from these layers, on each side of the pipe.

A change of behaviour dependent on  $\Lambda$  is not unprecedented. Hino *et al* [4] showed that the onset of turbulence in the reciprocating flow in a very long pipe, where end effects were eliminated, was a function only of  $Re_{\delta}$  for  $\Lambda > 2$ . However, the fact that the more complicated flow through the open-ended pipe still follows a similar pattern is novel.

Figure 5 attempts to address the applicability of these results to the application of HFV. The airway is essentially a set of pipes connected via bifurcations. A bifurcation here is the point at which a large pipe splits into two smaller pipes. The structure is almost self-similar, at least down to generation 15 (where the trachea is the first generation). The ratio of the lower to upper pipe diameters at a given bifurcation is  $d_2/d_1 = 0.79$ , and each pipe section has a length of around three diameters [2]. In a paper assessing different ventilators, Harcourt *et al* [3] used typical clinic parameters of a volume per inhalation of 6ml, a frequency of 10Hz and an endotracheal tube of internal diameter 3.5mm. Using these numbers (and assuming the internal diameter of the endotracheal tube is the diameter of the first airway generation) allows  $Re_{max}$  and  $\Lambda$  to be calculated at each generation, and it is these parameters plotted in figure 5.

This plot illustrates two primary features of this flow: first, all generations have reasonably low values of  $\Lambda$ , with even the highest value obtained in the trachea being  $< 2.5$ . This indicates that all generations are likely to operate in the low  $\Lambda$  regime. Second, that the middle generations around 8 and 9 have parameters close to the optimum for the low  $\Lambda$  regime identified in figure 2. This indicates that understanding mean streaming that forms in these flows is likely to aid in understanding the overall gas transport through these middle generations.

## Conclusions

The reciprocating flow in a straight pipe with a free end exiting in a large reservoir has been investigated. This flow has been used as a very basic model of the fluid mechanics, in par-

ticular the nonlinear mean streaming, that occurs during high-frequency ventilation. It has been shown that the flow can be classified into two basic regimes: a low  $\Lambda$  regime where the flow is essentially independent of  $\Lambda$  and the recirculating flux has a local maxima at a value of  $Re_{max} \simeq 300$ , and a high  $\Lambda$  regime where again the flow is independent of  $\Lambda$  and the recirculating flux is a weak linear function of  $Re_{max}$ . A simple consideration of the airway geometry has shown that most of the airway should operate in the low  $\Lambda$  regime, and that the middle generations operate around the optimum conditions for maximum recirculating flux.

## Acknowledgements

This work was supported financially through the Australian Research Council Discovery Project DP150103177. Computations were conducted under competitive grant NCIZ4 from the National Computational Merit Allocation Scheme, and at the Swinburne Centre for Astrophysics and supercomputing.

## References

- [1] Chatwin, P., On the longitudinal dispersion of passive contaminant in oscillatory flows in tubes, *J. Fluid Mech.*, **71**, 1975, 513–527.
- [2] Grotberg, J., Pulmonary flow and transport phenomena, *Ann. Rev. Fluid Mech.*, **26**, 1994, 529–571.
- [3] Harcourt, E. D., John, J., Dargaville, P. A., Zannin, E., Davis, P. G. and Tingay, D. G., Pressure and flow waveform characteristics of eight high-frequency oscillators, *Pediatric Critical Care Medicine*, **15**, 2014, e234–e240.
- [4] Hino, M., Sawamoto, M. and Takasu, S., Experiments on transition to turbulence in an oscillatory pipe flow, *J. Fluid Mech.*, **75**, 1976, 193–207.
- [5] Leontini, J., Thompson, M. and Hourigan, K., Three-dimensional transition in the wake of a transversely oscillating cylinder, *J. Fluid Mech.*, **577**, 2007, 79–104.
- [6] Rimensberger, P., ICU Cornerstone: High frequency ventilation is here to stay, *Critical care*, **7**, 2003, 342–345.
- [7] Slutsky, A. and Brown, R., Cardiogenic oscillations: a potential mechanism enhancing oxygenation during apneic respiration, *Medical Hypotheses*, **8**, 1982, 393–400.
- [8] Standiford, T. and Morganroth, M., High-frequency ventilation, *Chest*, **96**, 1989, 1380–1389.
- [9] Taylor, G., Dispersion of soluble matter in solvent flowing slowly through a tube, *Proceedings of the Royal Society A*, **219**, 1953, 186–203.
- [10] Thompson, M., Hourigan, K. and Sheridan, J., Three-dimensional instabilities in the wake of a circular cylinder, *Exp. Therm. Fluid Sci.*, **12**, 1996, 190–196.
- [11] Womersley, J., Method for the calculation of velocity, rate of flow and viscous drag in arteries when the pressure gradient is known, *Journal of Physiology*, **127**, 1955, 553–563.